Structure of Starch-Sepiolite Bio-Nanocomposites: Effect of Processing and Matrix-Filler Interactions

A SYNTHETIC METHOD FOR ASSESSING THE RISK OF DAM FLOODING*

S. Grimaldi
(PhD Student, DITIC, Politecnico di Torino, Italy)

D. Poggi
(Professor, DITIC, Politecnico di Torino, Italy)

1. INTRODUCTION

Risk analysis concepts for evaluation of existing dams safety have been widely studied and applied in the last three decades (Gruetter and Schnitter [1]; US Bureau of Reclamation [2]; Salmon and Hartford [3]; Hartford and Nielsen [4]). They are becoming increasing popular to assist dam owners and public authorities in a) decision making to obtain maximum benefit from investment of limited resources, and b) territorial management planning for assessing the economic damage as a result of the flooding. Nevertheless, risk-based methods are often very expensive in terms of time, manpower, and data entry. The large number of small and medium dams built in Europe requires a synthetic methodology based on very little data entry in order to limit costs. This paper presents a simple, but scientifically based, analytical procedure to estimate dam-break flooding intensity and to assess risk of small and medium dam flooding.

2. RISK DEFINITION

According to a widely accepted definition risk is the conditional probability of the magnitude of harm attendant on exposure to a perturbation. Eq. [1] is a simple expression for risk : hazard H, vulnerability V and potential damage D are the key parameters,

$$R = H \cdot V \cdot D \qquad [1]$$

Hazard is the probability of occurrence of a potentially damaging phenomenon; it depends on structural properties, maintenance and managing plans, geographical and hydrological conditions: it is an intrinsic parameter which evaluation requires specific analyses and will not be discussed in this paper.

* Une méthode synthetique d'estimation du risque associé à la rupture d'un barrage

Vulnerability is the degree of loss resulting from the occurrence of the phenomenon; it s a function of both flood wave intensity and ability of the elements at risk to face the dam-break. In particular, flow velocity (*v)* and maximum water depth (*y)* may be used to estimate flood intensity. Experimental studies (Black [5], Abt et al.[6], USACE [7], Clausen and Clark [8], Karvonen et al. [9]) showed that the boundaries between damage categories (such as complete, major, and minor destruction) can be delineated by curves of constant damage where the key parameter is the damage parameter value *vy* (m^2/s).
A rapid procedure intended to define synthetic index may be based on few vulnerability levels; referring to urban areas they are:

V_{100} : complete destruction (i.e. loss of 100%), $vy = 7\ m^2/s$;
V_{70} : major destruction (i.e. loss of 70%), $vy = 3\ m^2/s$;
V_{30} : minor destruction (i.e. loss of 30%), $vy = 1\ m^2/s$.

Potential damage is the total amount of both direct and indirect losses due to the phenomenon occurrence; its evaluation requires listing of all downstream elements swept by the flood wave. This approach requires an extremely detailed knowledge of downstream land use. The potential damage is obtained by summing up the value of all the elements at risk.

As a consequence of the large number of medium and small dams built in Europe, the use of this strict approach causes unacceptable costs in terms of both money and time. In order to adopt a rapid procedure based on very little data entry a simpler risk definition has been proposed:

$$R = H \cdot V \cdot E \qquad [2]$$

In Eq. [2] a qualitative evaluation of elements value (E) replaces the potential damage (D). Referring to capital goods a qualitative evaluation of both direct and indirect losses can be easily achieved by means of a land use map of the downstream valley: different land use classes obviously involve different exposure levels.
Three exposure levels may be used for a qualitative risk zonation:

E1: unhabitated or non-productive areas;
E2: rural areas, secondary communication lines, parks;
E3: urban and touristic areas; plants; highly important roads and railways.

3. BASIC EQUATIONS

As stated before, decision support procedure requires the evaluation of flood intensity in each cross section *x* far downstream of the dam. The product *v(x)y(x)* is the key parameter to assess the consequence of possible dam break in terms of economical damages. This product can be roughly written as the ratio between the maximum flow rate q_{max} *(x)* and some length scale of the cross

section width *b* (Eq. [3]), as a consequence the main parameter needed to estimate flood intensity at each cross section *x* is $q_{max}(x)$.

$$v(x)y(x) = \frac{q_{\max}(x)}{b(x)} \qquad [3]$$

Dam break wave modeling is thus extremely important in providing the information needed for risk assessment and management of river valleys. Since analytical as well as experimental modeling both refer to very simple scenarios and badly fit real cases, in recently years the emphasis has shifted toward numerical solutions.

A dam break wave is the flow resulting from a release of a mass of fluid in a channel witch generates a flood wave propagating in the tail water valley and a negative wave propagating up along the reservoir. The streamwise length scale of the motion is usually assumed to be much greater than the depth of the intruding current, so that the vertical fluid accelerations are negligible and the pressure is hydrostatic to leading order. With the further assumptions that drag forces may be neglected and that the current does not mix with the ambient, the motion may be modeled by the shallow water equations (Whitham [10]). Thus aligning the x-axis with the direction of propagation and denoting the downstream cross section area with Ω , the flow depth and discharge by *h* and *q*, respectively, we find that

$$\begin{cases} \dfrac{\partial q}{\partial x} + \dfrac{\partial \Omega}{\partial t} = 0 & [4a] \\ \dfrac{1}{\Omega}\dfrac{\partial q}{\partial t} + \dfrac{1}{\Omega}\dfrac{\partial}{\partial x}\left(\dfrac{q^2}{\Omega}\right) + g\dfrac{\partial y}{\partial x} - gi_f - gj = 0 & [4b] \end{cases}$$

Local acceleration term	Convective acceleration term	Pressure force term	Gravity force term	Friction force term

where i_f is the bed slope and *j* is the friction slope. Equations [4] derive from the principles of continuity [4a] (conservation of mass) and momentum [4b] (essentially, Newton's second law of motion).

The shallow water equations [4] cannot be solved analytically because of nonlinear terms, e.g. the friction slope *j* . A numerical modeling scheme is based on approximate solution techniques and is validated by experimental or real data sets.

In particular, we used the numerical code *BreZo 4.0* due to Begnudelli & Sanders [11]. *BreZo 4.0* solves the shallow-water equations using a Godunov-type finite volume algorithm that runs on an unstructured grid of triangular cells and was optimized for wet and dry conditions. By means of this software forecasts of the flood wave under different hypothesis can be set up, simulated and analyzed.

4. MODELS DESCRIPTION

A physically based study on dam break flood routing parameters involves the definition of many simple but representative models of both dams and downstream valleys features. Hence very little information is often available, a suitable methodology must require few parameters. A proper analysis of Piedmontese dams and valleys features allowed to build many simple but representative models.

Reservoir geometry: Both numerical and experimental dambreak studies usually use wedge shaped reservoirs whose bed slope equals downstream valley slope i_f, nevertheless our analysis highlighted that a parallelepiped can properly fit several reservoirs shape.
A shape coefficient k was defined as the ratio between measured a_{ms} and modeled a_{md} values of basin area a (Eq.[5])

$$k = \frac{a_{ms}}{a_{md}} \qquad [5]$$

Modeled area values a_{md} are computed as the ratio between reservoir volume and height values: $a_{ms}=v/y_o$.
Referring to many simple solids, the shape coefficient k equals 0.75 for an ellipsoid quarter, 1 for a parallelepiped, 1.5 for a rectangular based pyramid, 2 for a wedge, 3 for a triangular based pyramid.
Based on the database supplied, the probability density function of k values pointed out that the largest fraction of Piedmontese dams has a parallelepiped shape. Fig. 1 shows the Piedmontese reservoir shape probability density frunction curve.

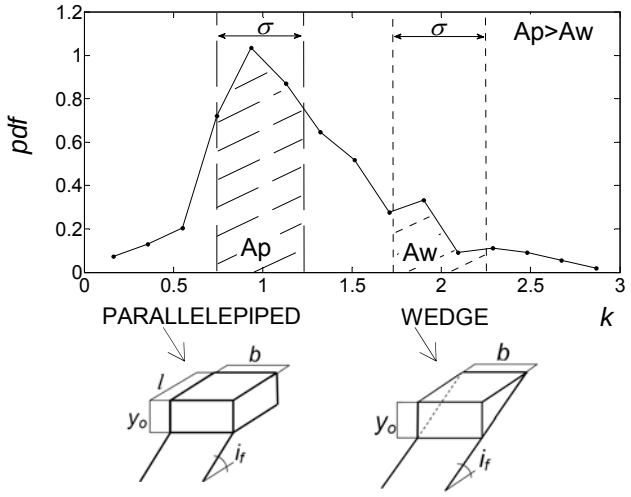

Fig. 1
Piedmontese reservoirs shape probability density curve
Courbe de densité de probabilité de la géométrie des barrages du Piémont

Despite the former hypothesis of a wedge shaped reservoir, one more parameter, i.e. the reservoir length l , is required in addition to dam height y_o and width b values in order to completely define the geometry of a parallelepiped-shaped reservoir. On the basis of a statistic analysis of Piedmontese reservoirs typical upstream length l, dam height y_o and width b were used in order to build our numerical lab.

Downstream land morphology: To minimize the natural flood wave attenuation effect a downstream prismatic channel with constant width b_{valley} , uniform slope i_f and roughness n was used. Their values were defined using statistic analyses of the Piedmontese downstream land features.

Dam-break mechanism: Dams can fail gradually or instantaneously, totally or partially. The mechanism depends both on the cause of failure and on the dam type. An instantaneous failure constitutes the worst scenario. It allows extreme events modeling and prescribes the upper bounds for the expected damages. Since the baseflow in such a case can often be neglected, the dam-break wave propagates over a dry bed. The dam removal may be total, that is a large portion or the entire dam is removed, or partial, that is a small portion of the dam is removed determining the formation of a breach which width is b_{breach} .In this paper, both partial and total collapse will be analyzed.

Fig. 2 shows a scheme of the models implemented.

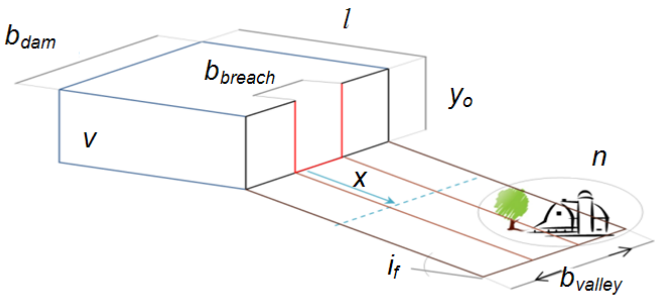

Fig.2.
Scheme of the models used
Schéma des modèles utilisés

5. TOTAL FAILURE

An instantaneous, total failure constitutes the worst scenario. It allows extreme events modeling and prescribes the upper bounds for the expected damages.

When the dam is instantaneously removed a series of negative waves route upward while a series of positive waves move downstream. The motion is

unaffected by the finite length *l* of the reservoir until the first backward-propagating wave has reached the rear of the lock. Thereafter the flow becomes affected by the finite basin length. As far as the first negative wave reaches the reservoir upstream cross section, it is reflected downstream. Whenever the disturbance due to the reservoir finite length catches up with the front wave, it affects the flood wave routing both in terms of arrival time and peak discharge values. In particular, it reduces both flood wave celerity and intensity.

Using *BreZo 4.0* and the information of the Piedmontese dams a numerical lab was built to investigate dam break flood wave routing main parameters, i.e. negative, positive wave, and peak discharge celerity as well as peak discharge values.

5.1 WAVE TIME ARRIVAL

5.1.1 Negative wave celerity

The simple reservoir morphology with a constant depth yields to a constant value of the negative front wave celerity c_{NF} depending exclusively on the dam heigh h_o [6]:

$$c_{NF} = \sqrt{g \cdot y_o} \qquad [6]$$

Our numerical lab yielded to an identical result to that proposed by Ritter (1892).

5.1.2 Front wave and peak discharge celerity

A dam failure flood hydrograph generally has a sharp rising limb with a very short interval between the initial discharge rise and the peak outflow. As a consequence the arrival time of a properly defined characteristic discharge value may represent both front wave and peak outflow arrival time. Referring to Lauber and Hager's experimental studies on the positive wave celerity [12], we defined the characteristic discharge value q_c as a fraction of the maximum outflow at the dam site q_{dam} , i.e. the outflow at the dam site (*x=0*) at the collapse time (*t=0*):

$$q_c = 0.05 \cdot q_{dam} \qquad [7]$$

In case of total failure Ritter's analytical solution [13] allows q_{dam} evaluation, our numerical lab proved Eq. [8] effectiveness.

$$q_{dam} = \frac{8}{27} \cdot g^{\frac{1}{2}} \cdot b \cdot y_o^{\frac{3}{2}} \qquad [8]$$

5.1.3 *Infinite reservoir length*

As explained earlier the perturbation due to the reservoir finite length may affect the arrival time value. The implementation of a theoretical unlimited reservoir upstream length avoids the negative wave reflection at the upstream reservoir wall.

Referring to Piedmontese dams and valleys features we demonstrated that a total, instantaneous collapse involves, almost in its earliest phases, a supercritical flow. According to hydro-dynamics theory derivative terms of momentum equation (Eq. [4b]) in shallow water equations (Eq. [4]), i.e. acceleration and pressure terms, are negligible and friction and mass forces lead the motion. The resulting wave is called kinematic; the conceptually simpler kinematic model states that the flow is steady for momentum conservation while unsteady effects are taken into account through the continuity equation. The resulting quasi-linear hyperbolic differential system has analytical solutions. Referring to a rectangular prismatic channel Eq.[9] allows the evaluation of the celerity c_q of a constant discharge q.

$$c_q = \frac{dx_q}{dt} = \frac{1}{\alpha \cdot \left(\frac{n \cdot b^{2/3}}{i_f^{1/2}} \right) \cdot q^{-2/5}} \qquad [9]$$

Our numerical lab demonstrated Eq. [9] effectiveness in predicting the celerity of the characteristic discharge q_c provided that:

$$\alpha = \frac{3}{8} \qquad [10]$$

5.1.4 *Finite reservoir length*

A more realistic finite upstream length requires to focus on the disturbance due to negative waves upstream reflection and downstream routing. Fig. 3 shows the limited basin effect on flood hydrograph at the dam site.

Although curve "a_{dam}" has a monotone decreasing trend, curve "b_{dam}" shows a flex point and a concavity change. Curve "b_{dam}" lays on curve "a_{dam}" as far as at time t_l , i.e. as far as the first reflected negative wave reaches the dam site. For time t greater than t_l curve "b_{dam}" shows a concavity change and a downward translation. The reservoir depth attenuation neglectivity allows to evaluate the characteristic time t_l as [11]

$$t_l = \frac{2 \cdot l}{\sqrt{g \cdot y_o}} \qquad [11]$$

Since the reservoir is parallelepiped-shaped the first instant at which the flow is affected by the rear of the lock depends exclusively on dam height and basin length. For time t greater than t_l the disturbance generated by the rear of the lock travels downstream: as far as it reaches the front wave it affects the flood wave routing. In Fig. 3 curves "a_{max}" and "b_{max}" represent the peak discharge values evaluated at many downstream cross sections as a function of time. Provided that we replace the reservoir characteristic time t_l with a greater value t_D, curves "a_{max}" and "b_{max}" behave exactly like curves "a_{dam}" and "b_{dam}".

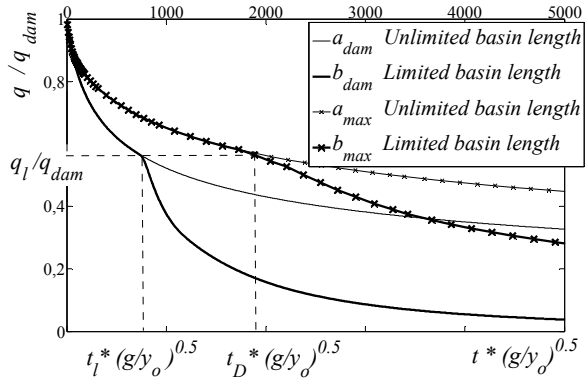

Fig. 3.
Limited basin effect
Influence de la longueur finie du reservoir

Fig. 4 shows the disturbance routing; as explained later we refer to the disturbance discharge as q_l . Obviously, although such disturbance has effects on each hydrograph, maximum discharge value is affected by reservoir emptying process despite that the laps of time employed by the negative wave to arrive at the basin upstream cross section, reflect and reach the cross section itself is smaller than the peak flow arrival time.

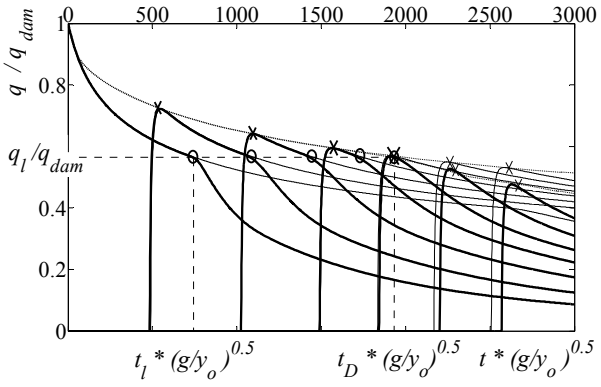

Fig. 4.
Reservoir emptying disturbance effect routing
Propagation de la perturbation due à le évidage du reservoir

Since diffusive terms, i.e. acceleration and pressure terms, of the momentum equation [4b] are negligible, mass and friction force terms lead the

quasi-steady motion and the kinematic model properly describes the flood wave routing. Hunt [14] showed how kinematic model can be used to obtain closed-form approximations; calculations and experiments suggested that these kinematic wave solutions become valid after the shock has traveled a number of reservoir lengths downstream.

Our numerical analyses pointed out that the disturbance discharge q_I is constant and equals dam site discharge value at time t_I.

Referring to the kinematic model, Eq. [9] allows the evaluation of the celerity of a constant discharge. Numerical efforts pointed out Eq. [9] effectiveness provided Eq. [12]

$$\alpha = \frac{3}{5} \qquad [12]$$

As stated so far, equations [9,10] and [9,12] respectively allow the evaluation of flood and disturbance wave celerities: Fig. 5 shows that point D (x_D, t_D) named detachment point is the only common solution. The detachment point *D* marks both the first instant and the nearest location to the dam at which the peak discharge is affected by the presence of the rear wall of the lock.

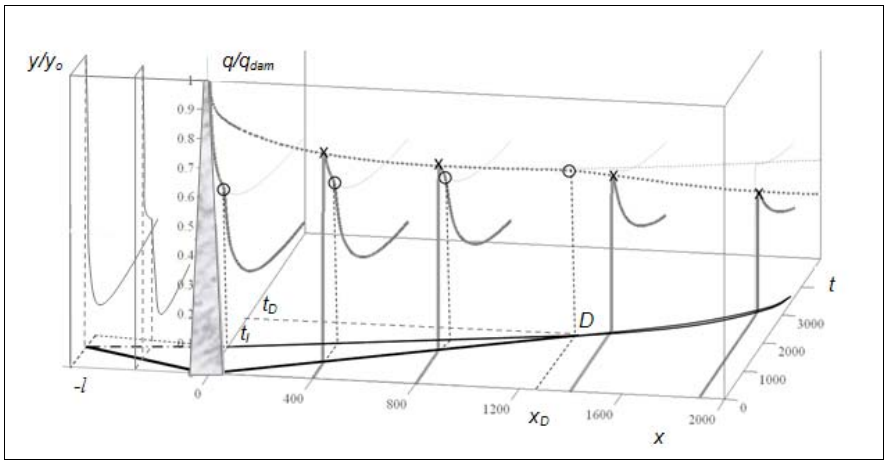

Fig. 5
Negative wave, characteristic discharge, and disturbance wave routing.
Propagation de l'onde negatif, du dèbit caractéristique, de la perturbation due à le évidage du reservoir

Obviously the assessment the reservoir emptying disturbance celerity requires the evaluation of the disturbance discharge value q_I. The assessment of the discharge value q_I requires the reservoir emptying equations. In case the flow is supercritical the downstream flood routing doesn't have any influence upstream and the reservoir geometric and hydraulic features, i.e. dam height and width and basin length and roughness, lead the emptying hydrograph. According to our analyses, for small times Dressler [15] theoretical solution fits numerical results (Eq. [15]). Referring to larger times our numerical lab yielded to Eq. [16], and Eq. [17]. The appendix lists the analytical equations pointed out.

The reservoir emptying perturbation makes the flood wave slow down and reduce its peak discharge values. Our numerical analyses highlighted that the dam height y_o as well as the basin length l are the flood routing leading parameters. Eq. [18] allows the evaluation of the flood wave celerity for times t greater than t_d and cross sections x farter than x_D from the dam site.

$$\frac{x - x_D}{l} = 0.370 \cdot \sqrt{g \cdot y_0} \cdot \frac{t - t_D}{l} \qquad [18]$$

5.2 MAXIMUM DISCHARGE VALUES

As mentioned earlier, flood wave intensity evaluation requires a procedure for estimating the maximum discharge at each cross section x far from the dam, q_{max} In the following, q_{max} will be normalized by q_{dam}, , i.e. the discharge value at dam site $x=0$ at failure time $t=0$. This approach allows us to focus on the factors affecting the wave attenuation effect. As mentioned earlier, according to both Ritter theoretical solution and our numerical analyzes Eeq. [8] allows q_{dam} evaluation.

5.2.1 Unlimited Reservoir Lenght

The implementation of a theoretical unlimited reservoir upstream length avoids the disturbance due to the wall at the rear of the lock and allows to focus on downstream valley parameters influence on peak discharge attenuation.

Numerical analyses pointed out that the ratio i_f/n^2 is the key parameter to describe the downstream land hydraulic features. Fig. 6 shows the normalized discharge values of an unlimited reservoir as a function of downstream cross section distance from the dam.

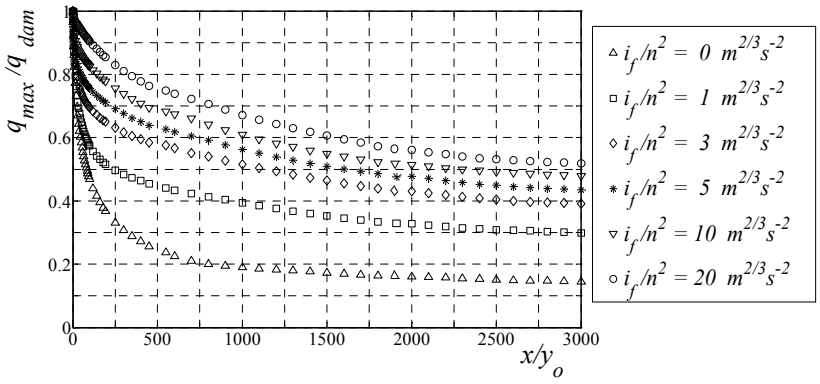

Fig. 6
Downstream land hydraulic influence on peak discharge attenuation
Influence de la géométrie du lit de la rivière sur le laminage du debit maximal

The smaller i_f/n^2 , the greater the influence of diffusive terms in momentum Eq. [4b], the larger the attenuation of the discharge hydrograph . All the curves plotted have a monotone decreasing behaviour. In particular, this behaviour

depends on downstream cross section distance x, dam height y_o , downstream land hydraulic features n, i_f (Eq.[19]); in general is:

$$\frac{q_{\max}}{q_{dam}} = f\left(\frac{x}{y_o}, \frac{i_f}{n^2}\right) \qquad [19]$$

5.2.2 Limited Reservoir Length

A more realistic finite upstream reservoir extension requires the introduction of the basin length l in Eq. [19].

As explained earlier (Fig. 3) curve "a_{max}" lays on curve "b_{max}" as far as the detachment point D, i.e. the cross section nearest to the dam affected by the disturbance due to the finite basin length. The disturbance wave makes the flood wave slow down; the second most noticeable effect is a sensible increase in the flood wave peak attenuation.

In case the downstream cross section distance x is greater than detachment point distance from the dam x_D, our numerical analyses pointed out downstream cross section distance x , basin length l, downstream valley roughness n, and slope i_f as the leading parameters of the flood wave attenuation. Moreover, sensible changes in dam height y_o have no influence on peak discharge. Eq. [20] reviews Eq. [19]:

$$\frac{q_{\max}}{q_{dam}} = f\left(\frac{x}{l}, \frac{i_f}{n^2}\right) \qquad [20]$$

Numerical efforts yielded to the analytical Eq. [21], [22].

$$x < x_D \Rightarrow \qquad \frac{q_{\max}}{q_{dam}} = \alpha \cdot \left(\frac{x}{y_o}\right)^{\beta} + \gamma \qquad \begin{cases} \alpha = -\dfrac{0.27}{0.30 \cdot \dfrac{i_f}{n^2} + 1} \\ \beta = \beta_1 \cdot \log\left(\dfrac{i_f}{n^2}\right) + \beta_2 \quad \begin{cases} \beta_1 = -0.00103 \cdot y_o + 0.08568 \\ \beta_2 = 0.01088 \end{cases} \\ \gamma = -\alpha + 1 \end{cases} \qquad [21]$$

$$x > x_D \Rightarrow \qquad \frac{q_{\max}}{q_{dam}} = \lambda \cdot \left(\frac{x}{l}\right)^{\delta} \qquad \begin{cases} \lambda = 0.96010 \cdot \log\left(\dfrac{i_f}{n^2} + 1\right) + 0.12780 \\ \delta = -1 \end{cases} \qquad [22]$$

6. PARTIAL FAILURE

6.1 BREACH AND DOWNSTREAM VALLEYS FEATURES

In case the collapse is partial the evaluation of the reservoir outflow peak discharge requires the breach geometry definition. Starting from the 1980's, several researchers compiled databases of well documented case studies in efforts to develop predictive relations for breach shape, formation time and peak outflow (Singh and Snorrason [16]; Froelich [17]; Fread [18]). According to a statistic analysis of a database developed by Wahl [19] containing a large number of case studies, the breach model can be assumed rectangular, it is as height as the dam and four times that value wide, i.e. $y_{breach} = y_o$ and $b_{breach}=4y_o$

A synthetic but complete modeling of downstream land morphology requires two antithetical settlings respectively representing large valleys (i.e. as wide as the dam) and narrow valleys (i.e. as wide as the breach). Fig. 7 shows hypothetical downstream territory geometries.

6.2 FLOOD WAVE ROUTING

A partial dam breach generates downward flood waves as well as upwards negative waves. Starting from the breach section, the first negative wave propagates upstream following a central path as far as the rear of the lock. The mass of water stoked at both sides take part in the reservoir emptying process after the first negative wave downward reflection. As a result of the breach dimensions, several reflected waves from upstream and dam section are observed. Whenever the disturbance due to the reservoir finite length catches up with the front wave, it affects the flood wave routing both in terms of arrival time and peak discharge values. As showed for the total failure, an unlimited reservoir extension yields to monotone decreasing values of the ratio q_{max}/q_{dam} as a function of the cross section distance x/y_o; on the contrary a limited reservoir extension yields to a flex point x_D and a concavity change due to reservoir emptying process

Referring to a total failure, a partial breach force the reservoir emptying process to slow down, as a consequence peak discharge attenuation as well as peak time arrival increase.

Since it is impossible to explain all details we limit the discussion on practical results. Referring to a narrow valley, i.e. as wide as the breach, our numerical analyzes pointed out that Eq. [9,10] crossed with Eq. [9,12] allow a proper assessment of the detachment point coordinates (x_D,t_D). A large valley, i.e. as wide as the dam, yields to a complex phenomenon, nevertheless our numerical lab proved that Eq. [9,10] crossed with Eq. [9,12] lead to conservative results, i.e. the real detachment point coordinate values are smaller than the predicted ones. The method proposed generally increases the laps of time as

well as the downstream distance from the dam not affected by the reservoir finite length, as a result real peak discharge values and arrival time are smaller than the predicted ones.

6.3 PEAK DISCHARGE VALUES

6.3.1 Peak discharge at dam site

As stated before, a first and crucial parameter for evaluating $q_{max}(x)$ is the maximum outflow at the dam site $q_{max}(x=0)$ *i.e.* q_{dam} . Generally, a breach section may be compared to a broad crested weir, and the outflow discharge may be evaluated, on the basis of fluid mechanics theory, as [23]:

$$q_{dam} = C_d b_{breach} y_o^{\frac{3}{2}} (2g)^{\frac{1}{2}} \qquad [23]$$

Where b_{breach} is the weir (breach) width; y_o represents the hydraulic head: since the dam removal is instantaneous it is equal to the dam height; g is the gravital acceleration; C_d is a discharge coefficient depending on weir geometry.
In case of total collapse b_{breach} equals b_{dam} and Ritter's analytical solution as well as our numerical results point out the discharge coefficient value [24]:

$$C_d = 0.21 \qquad [24]$$

In case of partial failure b_{breach} equals $4y_o$ and Eq. [23] turns out asEq. [25]

$$q_{dam} = 4C_d y_o^{\frac{5}{2}} (2g)^{\frac{1}{2}} \qquad [25]$$

Numerical results highlighted that the discharge coefficient C_D has a monotone increasing value: a total failure yields to the lower boundary value ([24]) while the upper boundary value equals the discharge coefficient value of a Belanger weir.
In particular, a good fitting of this behavior is given by Eq. [26] which includes both partial and total collapse.

$$C_d = 0.3310 \cdot \left(1 - 0.5100 \cdot e^{-0.0825 \left(\frac{b}{yo} \right)} \right) \qquad [26]$$

6.3.2 Limited Reservoir Length

As mentioned earlier flow rate through the breach assumes discharge characteristic of a broad-crested weir and relative breach dimension b/y_o leads the peak discharge at dam site.

Moreover, our analyses showed b/y_o is also the key parameter leading downstream flow attenuation, as a consequence Eq.[27] and Eq.[28] review Eq.[19] and Eq.[20].

$$x < x_D \Rightarrow \qquad \frac{q_{\max}}{q_{dam}} = f\left(\frac{x}{y_o}, \frac{b}{y_o}, \frac{i_f}{n^2}\right) \qquad [27]$$

$$x > x_D \Rightarrow \qquad \frac{q_{\max}}{q_{dam}} = f\left(\frac{x}{l}, \frac{b}{y_o}, \frac{i_f}{n^2}\right) \qquad [28]$$

Let us briefly analyze the influence of a) the relative breach dimension b/y_o, and b) the downstream valley width b_{valley} on downstream peak discharge attenuation. Fig. 7 and 8 show the behavior of q_{max}/q_{dam} as a function of the normalized downstream cross section distance *x/l*.

Fig. 8 points out that the greater b/y_o, the lower the flood attenuation effect. This effect is not unexpected, in fact for large b/y_o the breach behaves as a leak and the reservoir emptying is a very slow process .

Fig. 7 shows that, as expected, the wider the valley, the greater the peak flow attenuation.

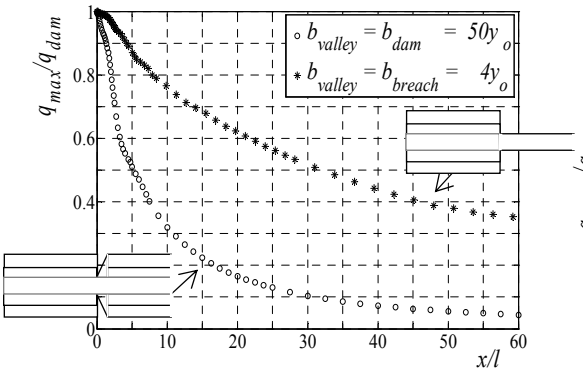

Fig. 7
Downstream valley width influence
Influence de la géométrie du lit de la rivière

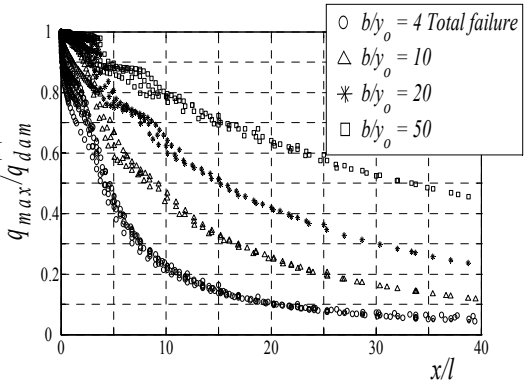

Fig. 8
Breach width influence
Influence de la largeur de la brèche

Narrow Valleys. As far as the flex point *d* reservoir maximum discharge is negligible and almost insensitive to breach dimension (18).

$$x < x_d \Rightarrow \frac{q_{\max}}{q_{dam}} = 1 \qquad [29]$$

As done for the total collapse, q_{max} may be parameterized for the partial collapse as [30]:

$$x > x_D \Rightarrow \quad \frac{q_{\max}}{q_{dam}} = \alpha_{P1} \cdot \frac{x}{l}^{\beta_{P1}} \quad \begin{cases} \alpha_{P1} = A_{P1} \cdot \log\left(\frac{i_f}{n^2} + 1\right) + B_{P1} \\ \beta_{P1} = 0.2137 \cdot \log\left(\frac{b}{y_o}\right) - 1.2856 \end{cases} \quad \begin{cases} A_{P1} = -0.00358 \cdot \frac{b}{y_o} + 0.9731 \\ B_{P1} = 0.00798 \cdot \frac{b}{y_o} + 0.0960 \end{cases} \qquad [30]$$

When b/y_o = 4 Eq. [30] obviously collapses to Eq. [22].

Large Valleys. Also in this case, as far as the flex point *d,* the attenuation of q_{max} is negligible and almost insensitive to breach dimension ([31]).

$$x < x_d \Rightarrow \frac{q_{\max}}{q_{dam}} = 1 \qquad [31]$$

Similarly to the narrow valleys case, q_{max} may be parameterized as [32]:

$$x > x_D \Rightarrow \quad \frac{q_{\max}}{q_{dam}} = \alpha_{P2} \cdot \frac{x}{l}^{\beta_{P2}} \quad \begin{cases} \alpha_{P2} = A_{P2} \cdot \log\left(\frac{i_f}{n^2} + 1\right) + B_{P2} \\ \beta_{P2} = 0.1656 \cdot \log\left(\frac{b}{y_o}\right) - 1.2128 \end{cases} \quad \begin{cases} A_{P2} = -0.1286 \log\left(\frac{b}{y_o}\right) + 1.119 \\ B_{P2} = 0.0032 \cdot \frac{b}{y_o} + 0.1201 \end{cases} \qquad [32]$$

7. VULNERABILITY DISTANCE

As explained so far, Eq.[19] to Eq. [32] yield to the assessment of the product *vy* at each cross section *x* of the downstream valley. Now we are interested in defining simple equations to predict how far from the dam a degree of damage is expected.

As explained earlier referring to urban areas the equations required should allow to locate the vulnerability threshold distances $x_t(vy)$ corresponding to the damage parameter *vy* values *7, 3, 1* m^2/s (see section 2)

Based on the element at risk susceptibility, the degree of damage accepted, the failure mechanism, dam and downstream valley features, Table 1 lists the analytical equations for vulnerability threshold distance assessment.

Table 1.
Analytical equations for vulnerability threshold distance assessment

Dam break mechanism	Downstream territory width	Analytical equation for threshold vulnerability distance	Eq.
TOTAL (instantaneous) FAILURE	$b_{valley} = b_{dam}$	$x_t = \left(\frac{vy}{\alpha_T C_d y_o^{\frac{3}{2}} \sqrt{2g}} \right)^{\frac{1}{\beta_T}} \cdot l$	[33] C_d [24] α_T [22] β_T [22]
PARTIAL (instantaneous) FAILURE	$b_{valley} = b_{breach}$ $b_{breach} = 4\, y_o$	$x_t = \left(\frac{vy}{\alpha_{P1} C_d y_o^{\frac{3}{2}} \sqrt{2g}} \right)^{\frac{1}{\beta_{P1}}} \cdot l$	[34] C_d [26] α_{P1} [30] β_{P1} [30]
	$b_{valley} = b_{dan}$ $b_{breach} = 4\, y_o$	$x_t = \left(\frac{vy}{4\alpha_{P2} C_d y_o^{\frac{3}{2}} \sqrt{2g}} \right)^{\frac{1}{\beta_{P2}}} \cdot l$	[35] C_d [26] α_{P2} [32] β_{P2} [32]

8. SUMMARY

Flood inundation due to dam failure may cause widespread damage to property, production, and infrastructure. Risk analysis concepts for evaluation of existing dams safety have been widely studied and applied in the last three decades (Federal Coordinating Council for Science, 1979; Gruetter and Schnitter, 1982; Atkinson and Vick, 1985; US Bureau of Reclamation, 1989; Nielsen, 1993; Salmon and Hartford, 1995; Hartford and Nielsen, 1995). Risk analyses are becoming increasingly popular to assist dam owners and public authorities in a) decision making to obtain maximum benefit from investment of limited resources, and b) territorial management planning for assessing the economic damage as a result of the flooding. Nevertheless, risk-based methods are often very expensive in terms of time, manpower, and data entry. This paper presents a simple, but scientifically based, analytical procedure to estimate dam-break flooding intensity and to assess risk of dams.

Here the risk of dam flooding is defined as the total economic damage caused by the failure of a specific structure and is evaluated on the basis of hazard, exposure, and vulnerability. Hazard is an intrinsic parameter of the dam and its evaluation requires specific analyses; exposure levels may be easily assessed by means of a land use map of the downstream valley; vulnerability evaluation requires a proper dam break flood wave modeling.

Dambreak wave analytical solutions available badly fit real cases while numerical modeling involves several data entry and a lot of time in order to analyze one structure. The large number of small and medium dams built in Europe requires a

proper synthetic methodology. Referring to Piedmontese dams (Italy), many representative but simple models of dams and valleys features have been built. The complete modeling of dam break wave routing was achieved using the hydraulic software BreZo 4.0. By means of this numerical lab the key parameters leading flood wave routing were pointed out. This paper proposes an original, simple, effective, synthetic, physically based on statistic analyses and hydraulic principles protocol to assess vulnerability parameter q_{max}/b (q_{max} is cross section peak discharge and b represent cross section width value).

An instantaneous, total failure constitutes the worst scenario and prescribes the upper bounds for the expected damages. A study on flood wave routing pointed out the key parameters as well as the analytical equations to assess vulnerability parameter values at each point downstream of the dam.

According to our numerical lab, the reservoir emptying process doesn't affect flood wave arrival time as well as peak discharge values despite the cross section distance from the dam is smaller than a threshold value. The key parameters leading dam break flood wave routing are cross section distance from the dam, dam width and height, downstream valley roughness and slope. Whenever the disturbance wave due to the reservoir emptying process catches up with the front wave the flood wave slows down and the peak discharge attenuation increases. Referring to cross section farter than the threshold value from the dam the key parameters are downstream cross section distance, basin length, dam width, downstream valley roughness and slope. The assessment of the position of the threshold distance depends both on reservoir geometry (i.e. basin length, dam height and width) and downstream land hydraulic parameters (i.e. roughness and slope), it was based on the evaluation of the reservoir emptying equations.

The hypothesis of an instantaneous, partial failure completed the analyzes. It required the definition of the breach parameters as well as a synthetic but complete modeling of downstream land morphology. Our lab pointed out flood wave routing mechanism; the reservoir emptying process affects flood wave routing despite downstream cross section distance is greater than the threshold value. In order to assess the threshold distance the method proposed for a total failure yields to conservative results. Both near and far cross section peak discharge assessment requires to add breach width value to the parameters listed previously. Numerical efforts yielded to proper analytical equations to assess peak discharge values at each cross section downstream of the dam.

Based on the failure mechanism, a few geometric and hydraulic parameters, and a simple land use map the synthetic method proposed herein allows the assessment of the total economical damage due to the possible failure of a structure.

L' inondation due à la rupture d'un barrage peut causer graves dommages aux biens matériels, aux infrastructures, aux activités productives. L'analyse du risque associé aux barrages existants a été largement développée et appliquée au cours dans les dernières trois décennies (Federal Coordinating Council for Science, 1979; Gruetter and Schnitter, 1982; Atkinson and Vick, 1985; US Bureau of Reclamation, 1989; Nielsen, 1993; Salmon and Hartford, 1995;

Hartford and Nielsen, 1995). L'analyse du risque est un instrument essentiel pour la gestion du territoire et pour la définition des priorités de l'intervention. Toutefois, elle est très coûteuse en termes de temps, capital, personnel technique nécessaire. Cet article présente une procédure analytique d'estimation du risque associé aux barrages, simple mais scientifiquement fondée.

Le risque est défini par le dommage économique total provoqué en aval à cause de la rupture d'un barrage et est fonction de la dangerosité, de l'exposition et de la vulnérabilité. La dangerosité est un paramètre intrinsèque caractéristique du barrage dont l'évaluation exige des preuves spécifiques; le niveau d'exposition peut être estimé simplement utilisant une carte représentant l'utilisation du territoire en aval; l'évaluation de la vulnérabilité exige la modélisation d'onde de rupture causée par l'effondrement du barrage. Les solutions analytiques de cette onde ne peuvent pas être utilisé aux fins de l'analyse des cas réels, néanmoins la modélisation numérique souvent exige longs délais, nombreux données d'entrée, l'utilisation du personnel technique hautement qualifié. Le grand nombre des barrages de petit et moyenne taille construits en Europe demande la définition d'une méthodologie synthétique fondée sur un petit nombre de paramètres d'entrée. Sur la base d'une analyse détaillée des barrages du Piémont (Italie) ont été construits des modèles simples mais représentatifs de la morphologie des réservoirs et des territoires en aval. La modélisation numérique de la propagation d'onde de rupture a été effectué utilisant le logiciel BreZo 4.0 . Ce laboratoire numérique a permis de détecter les paramètres géométriques et hydrauliques qui déterminent la valeur du paramètre de vulnérabilité q_{max}/b (q_{max} et b sont le débit maximal et la largeur de la section transversale en aval). L hypothèse rupture totale et instantanée permet de simuler les conditions les plus dangereux et fixe la limite supérieure de dommage économique total attendu. Une étude sur l'onde d'inondation a souligné les principaux paramètres ainsi que les équations pour évaluer les valeurs des paramètres de la vulnérabilité à chaque point en aval du barrage.

En ce qui concerne les analyses numériques réalisées, pour les sections les plus proches au barrage les valeurs du débit maximal et du relatif temps d'arrivée ne sont pas influencés par le vidange du réservoir et les paramètres d'intérêt sont la position de la section, l'hauteur du barrage, la rugosité et la pente du lit de la rivière. Au contraire, les valeurs relatifs aux sections les plus éloignées sont influencés par le vidange du réservoir et les paramètres d'intérêt sont la longueur du basin, la position de la section, la rugosité et la pente du lit de la rivière. Dans le détail, quand la perturbation générée par le vidange du réservoir atteint le front d'onde la rapidité de propagation diminue et, au contraire, l'effet de laminage du débit maximal augmente . Dans le cadre des analyses effectuées la distinction en sections "voisines" et "lointaines" est fonction des parameters du lit et du barrage et il a demandé la définition d'équations de vidange du réservoir.

L'enquête a été complétée en supposant une rupture partielle et instantané du serrement. L'analyse statistique de numéraux cas réels a permis la définition d'une géométrie de la brèche simplifiée. Un modelage synthétique mais complet des vallées réelles a demandé la définition de morphologies différentes pour le territoire en aval. Les analyses ont souligné un mécanisme de propagation de

l'inondation tout analogue au cas de rupture total. En particulier, pour la distinction en sections "voisines" et "lointaines", on propose, car precautionel, la méthode élaborée dans le cas précédent. Relativement à l'estimation des valeurs du pic de inondation en correspondance du barrage et de chaque section située en aval il faut d'ajouter aux modèles énumérés ci-dessus la largeur de la brèche.

Finalement, supposée la modalité de rupture, connus les caractéristiques géométriques et hydrauliques du réservoir et du territoire, définie le niveaux d'exposition, il se propose une méthodologie synthétique mais basés sur analyses scientifiques pour l'estimation du dommage économique total causé par la possible rupture d'un barrage .

9. APPENDIX

In order to assess analytical equations for dam site hydrograph we normalized discharge values $q(x=0,t)$ and time values *t* according to Dressler theory (Eq.[13], Eq.[14]).

$$Q(x=0,t)=\frac{q(x=0,t)}{q_{dam}} \quad [13] \qquad ; \qquad T=t\cdot\sqrt{\frac{g}{h_o}} \quad [14]$$

Table 2.
Analytical equations for dam site hydrograph assessement

Discharge value	Equations
$1 \geq Q(x=0,t) \geq 0.82$	$Q(x=0,t)=1-0.239\cdot\frac{g}{\chi^2}\cdot T$ [15] $\chi=\frac{1}{n}\cdot y_o^{1/6}$
$0.82 \geq Q(x=0,t) \geq 0.42$	$Q(x=0,t)=\alpha_2\cdot T^{\beta_2}$ [16] $\alpha_2=\gamma_2\cdot n^{\delta_2}$ $\begin{cases}\gamma_2=0.042591\cdot\log(h_o)+0.4401\\ \delta_2=-0.5300\end{cases}$ $\beta_2=-0.2667$
$Q(x=0,t) \leq 0.42$	$Q(x=0,t)=\alpha_3\cdot T^{\beta_3}$ [17] $\alpha_3=\gamma_3\cdot n^{\delta_3}$ $\begin{cases}\gamma_3=0.05154\cdot\log(h_o)+0.4570\\ \delta_3=-0.6300\end{cases}$ $\beta_3=-0.3200$

REFERENCES

[1] GRUETTER F., SCHNITTER N. J. Analytical risk assessment for dams. *International Commission on Large Dams, Proceedings 14, International Congress on Large Dams, Rio de Janeiro, Brazil.* 1982.

[2] US BUREAU OF RECLAMATION. Policy and proceedings for dam safety modification decision making.1989.

[3] SALMON G.M,; HARTFORD D.N.D. Rsk analysis for dam safety. *International Water Power and Dam Safety.* 1995.

[4] HARTFORD D. N. D., NIELSON, N. M. , GAFFR, D. C. Consequence-based dam safety, a balanced risk approach. *Waterpower '95*, Vol 3, San Francisco.

[5] BLACK R.D. Flood proofing rural residences. *A Project Agnes Report, Pennsylvania. New York State Coll. of Agriculture and Life Sciences*. 1975.

[6] Abt, S.R.; Wittler, R.J.; Taylor, A.; Love, D.J. April 1989. "Human stability in a high flood hazard zone". *Water resources bulletin*, American Water Resources Association.

[7] US ARMY CORPS OF ENGINEERS. Flood damage analysis package: users manual. USACE, Hydraulic Engineering Centre, Davis, CA. 1988

[8] CLAUSEN L., CLARK P.B. The development of criteria for predicting dambreak flood damages using modeling of historical dam failures. *International Conference on River Flood Hydraulics (edited by W. R. White).* 1990.

[9] KARVONEN T.,HEPOJIKI A.,HUHTA H.,KOTOLA J.,LOUHIO A. *RESCDAM. 2000*. Final report of Helsinki University of Technology - The use of physical models in dam-break flood analysis . 2000.

[10] WHITHAM G. B. *Linear and Nonlinear Waves*. Wiley. 1974.

[11] BEGNUDELLI L., BRADFORD, S.; SANDERS, B. "Adaptive Godunov-Based Model for Flood Simulation". *Journal of Hydraulic Engineering,* 2008.

[12] LAUBER G., HAGER W. Experiments to dambreak waves: horizontal channel. *Journal of Hydraulic research*. 1998.

[13] RITTER A. The propagation of water waves. *V.D.I. Zeitscher (Berlin)*. 1892.

[14] HUNT B. Perturbation solution for dam-break floods. *Journal of Hydraulic Engineering*. 1984.

[15] DRESSLER R.F. Hydraulic resistance effect upon the dam-break functions. *Journal of Research of the National Bureau of Standards*. 1952

[16] SINGH K. P., SNORRASON A. Sensitivity of outflow peaks and flood stages to the selection of dam breach parameters and simulation models. *Journal of Hydrology*. 1984

[17] FROEHLICH D.C. Embankment-Dam Breach Parameters. *Hydraulic Engineering, Proceedings of the 1987 ASCE National Conference on Hydraulic Engineering, Williamsburg, Virginia, August 3-7*, 1987.

[18] FREAD D.L. BREACH: an erosion model for earthen dam failures. *National Weather Service, National Oceanic and Atmospheric Administration, Silver Spring, Maryland*. 1988 (revised 1991).

[19] WAHL T. L. Prediction of embankment dam breach parameters - a literature review and needs assessment. *Dam Safety Report No.DSO-98-004 U.S. Dept. of the Interior, Bureau of Reclamation, Denver*. 1998.

Keywords: dam break wave, risk assessment, synthetic methodology, numerical analysis, hydraulic and geometric properties.